

RESEARCH PAPER

Transcriptome analysis reveals rice *MADS13* as an important repressor of the carpel development pathway in ovules

Michela Osnato^{1,2}, Elia Lacchini^{1,3}, Alessandro Pilatone¹, Ludovico Dreni^{1,4}, Andrea Grioni¹, Matteo Chiara¹, David Horner¹, Soraya Pelaz^{2,5}, and Martin M. Kater^{1,*}

¹ Department of Biosciences, University of Milan, Via Celoria 26, 20133 Milano, Italy

² Centre for Research in Agricultural Genomics (CRAG), CSIC-IRTA-UAB-UB, Campus UAB, Barcelona, Spain

³ VIB Center for Plant System Biology, Ghent, BELGIUM

⁴ Instituto de Biología Molecular y Celular de Plantas, Consejo Superior de Investigaciones Científicas-Universidad Politécnica de Valencia, Valencia, Spain

⁵ Institució Catalana de Recerca i Estudis Avançats (ICREA), Barcelona, Spain

* Correspondence: martin.kater@unimi.it

Received 15 June 2020; Editorial decision 24 September 2020; Accepted 3 October 2020

Editor: Zoe Wilson, University of Nottingham, UK

Abstract

In angiosperms, floral homeotic genes encoding MADS-domain transcription factors regulate the development of floral organs. Specifically, members of the *SEPALLATA* (*SEP*) and *AGAMOUS* (*AG*) subfamilies form higher-order protein complexes to control floral meristem determinacy and to specify the identity of female reproductive organs. In rice, the *AG* subfamily gene *OsMADS13* is intimately involved in the determination of ovule identity, since knock-out mutant plants develop carpel-like structures in place of ovules, resulting in female sterility. Little is known about the regulatory pathways at the base of rice gynoecium development. To investigate molecular mechanisms acting downstream of *OsMADS13*, we obtained transcriptomes of immature inflorescences from wild-type and *Osmads13* mutant plants. Among a total of 476 differentially expressed genes (DEGs), a substantial overlap with DEGs from the *SEP*-family *Osmads1* mutant was found, suggesting that *Osmads1* and *OsMADS13* may act on a common set of target genes. Expression studies and preliminary analyses of two up-regulated genes encoding Zinc-finger transcription factors indicated that our dataset represents a valuable resource for the identification of both *OsMADS13* target genes and novel players in rice ovule development. Taken together, our study suggests that *OsMADS13* is an important repressor of the carpel pathway during ovule development.

Keywords: Floral meristem determinacy, gynoecium, *Oryza sativa*, ovule, transcription, rice.

Introduction

In the majority of angiosperms studied to date, the formation of different floral organs in four concentric whorls is genetically controlled by five classes of transcription regulators (reviewed by Bowman *et al.*, 2012). The ABCDE model suggests that A- and B-class transcription factors (TFs) determine the development of sepals and petals in the outermost whorls, whilst

B- and C-class TFs control the formation of stamens and carpels in the innermost whorls (Causier *et al.*, 2010). Additional D-class factors exert their function in the formation of the ovule, the specialized sporophytic structure enclosing the female gametophyte which, upon fertilization, gives origin to the seed (Pinyopich *et al.*, 2003; Dreni *et al.*, 2007). Finally, E-class factors are required for the development of all floral structures and represent a molecular hub, as they mediate the formation of homo/heteromeric regulatory complexes composed of different combinations of the A-, B-, C-, and D-class factors specific to each of the four whorls (Malcomber and Kellogg, 2005). The majority of these floral homeotic proteins belong to the MADS-domain family and have been proposed to operate as quartets (two interacting dimers; reviewed by Theißen and Saedler, 2001) that bind two *cis*-regulatory elements, known as CArG-boxes, in the promoters of the genes that they regulate (Egea-Cortines *et al.*, 1999; Mendes *et al.*, 2013). This genetic model is broadly conserved across flowering plants, although variations are associated with a range of flower morphologies (Theissen and Melzer, 2007).

In the model species *Arabidopsis thaliana*, the floral meristem (FM) gives rise to four sepals, four petals, six stamens, and two fused carpels. Four E-class factors, SEPALLATA (SEP) 1, SEP2, SEP3, and SEP4, act redundantly to determine the identity of all floral organs (Pelaz *et al.*, 2000; Ditta *et al.*, 2004), and a complex composed of the E-class factor and the C-class factor AGAMOUS (AG) specifies the identity of stamens and carpels, and controls FM determinacy (Bowman *et al.*, 1989). The FM is consumed during flower development as AG regulates the shift towards organogenesis by mediating direct and indirect repression of the stem cell identity gene *WUSCHEL* (*WUS*) in the FM (Laux *et al.*, 1996; Brand *et al.*, 2000; Schoof *et al.*, 2000; Sun *et al.*, 2009; Liu *et al.*, 2011).

In the Arabidopsis genome, three additional *AG-like* genes—*SHATTERPROOF1* (*SHP1*), *SHP2*, and *SEEDSTICK* (*STK*)—are named after their function in seed dispersal (Liljegren *et al.*, 2000; Pinyopich *et al.*, 2003; Balanzà *et al.*, 2016). Although *STK* is specifically expressed in the pistil and ovules, the loss of its function only affects the formation of funiculi (Pinyopich *et al.*, 2003; Mizzotti *et al.*, 2014). However, integuments are converted into carpelloid structures in the *shp1 shp2 stk* triple-mutant, indicating that the three genes act redundantly in the determination of ovule identity (Pinyopich *et al.*, 2003; Brambilla *et al.*, 2007). Interestingly, the formation of carpel-like organs in the place of ovules is also observed in the *sep1 sep2 sep3/+* triple-mutant (Favaro *et al.*, 2003), demonstrating that these factors are crucial for a correct reproductive development. At the molecular level, *STK*, *SHP1*, and *SHP2* redundantly control the expression of *VERDANDI* (*VDD*), a gene encoding a B3-domain TF involved in the development of antipodal cells and synergids (Matias-Hernandez *et al.*, 2010). Specifically, the *STK*–*SEP3* dimers bind two nearby CArG boxes in the

promoter of *VDD*, inducing the formation of a loop that results in the activation of *VDD* in the female gametophyte (Mendes *et al.*, 2013). In the pistil, *STK* interacts with NO TRANSMITTING TRACT (NTT) to control the early events of gynoecium development and septum function, which is important for fertilization (Herrera-Ubaldo *et al.*, 2019). In addition, *STK* also plays a role in fruit development by regulating the cytokinin hormonal pathway, thus controlling fruit size (Di Marzo *et al.*, 2020).

In grasses, the duplication and diversification of *MADS-box* genes is probably associated with the origin and diversification of flower morphology (the spikelet; Malcomber and Kellogg, 2004). In rice (*Oryza sativa*), the floret meristem differentiates the palea and lemma, two lodicules (equivalent to petals), six stamens, and a central carpel containing a single ovule (Itoh *et al.*, 2005). Among the five *SEP-like* genes in the rice genome, the *OsmADS1* loss-of-function mutant, originally described as *leafy hull sterile 1* (*lhs1*), displays defects in both flower development and FM determinacy, and resembles E-class function mutants (Jeon *et al.*, 2000). Indeed, in *Osmads1* mutants, floral organs are converted into glume-like structures, and a spikelet-within-a-spikelet develops in the centre of the flower (Jeon *et al.*, 2000; Prasad *et al.*, 2001, 2005; Agrawal *et al.*, 2005; Hu *et al.*, 2015). Similar to Arabidopsis, the rice AG homologs *OsmADS3* and *OsmADS58* redundantly control the identity of reproductive organs (stamens and carpels) and meristem determinacy (Yamaguchi *et al.*, 2006; Dreni *et al.*, 2011). The AG-like factor *OsmADS13* also controls the determinacy of the FM and the identity of the ovule within the carpel, thus showing a class-D function, since *Osmads13* mutants display homeotic transformations of ovules into carpels (Dreni *et al.*, 2007, 2011).

Over the last decade, large-scale omics approaches have facilitated a deeper understanding of the gene regulatory networks that underlie flower development, particularly in Arabidopsis. ChIP-sequencing and transcriptomics analyses have helped in deciphering the transcriptional cascades downstream of the C-class factor AG (Ó'Maoiléidigh *et al.*, 2013) and the E-class factor SEPALLATA 3 (Kaufmann *et al.*, 2009). These studies suggest a function of AG in the promotion of gynoecium development via the activation of auxin biosynthesis (Ó'Maoiléidigh *et al.*, 2013; Yamaguchi *et al.*, 2017), and of SEP3 in the regulation of floral organ morphogenesis via auxin signalling pathways (Kaufmann *et al.*, 2009).

The combination of genome-wide DNA-binding assays and expression data has also indicated that the rice E-class factor *OsmADS1* activates genes in the auxin pathway involved in the differentiation of female reproductive tissues (Khanday *et al.*, 2013, 2016). Nevertheless, genetic and molecular studies suggest a complex interplay between rice floral homeotic factors (Li *et al.*, 2011; Hu *et al.*, 2015). Transcriptomic analyses have also provided valuable information regarding the different steps of male and female gamete development in rice (Tang

et al., 2010; Kubo *et al.*, 2013). However, little is known about the molecular mechanisms underlying the gene regulatory networks that control ovule development in rice.

In this study, we investigated changes in the modulation of gene expression between wild-type rice and the *Osmads13* mutant, and identified genes that were deregulated in developing *Osmads13* inflorescences. By comparing our datasets with those published for *OsMADS1* knock-down and knock-out mutants (Khanday *et al.*, 2013; Hu *et al.*, 2015) we identified interesting regulatory genes, and performed detailed expression analyses in specific cell types and functional characterization during reproductive growth. Taken together, our findings provide new insights into the early processes that regulate the formation of female reproductive organs. Based on these findings, we propose a genetic framework downstream of the D-class factor OsMADS13.

Materials and methods

Plant material and growth conditions

Rice (*Oryza sativa* L. subsp. *Japonica* cv. Dongjin) plants were grown under controlled long-day conditions in a chamber (16/8 h light/dark at 28/22 °C). After 8–10 weeks, plants were transferred to short-day conditions (10/14 h light/dark at 28/22 °C) to induce flowering. After 3 weeks, developing inflorescences (0.5–0.7 cm length) were harvested for expression analysis. As previously described by Itoh *et al.* (2005), this corresponded to the stages In6 and In7 of inflorescence development, Sp7 (carpel primordium) and Sp8 (ovule and pollen the latter) of spikelet development, and Ov1 of ovule development. After heading, mature flowers at anthesis were collected for phenotypic analysis.

In this study, we used the *Osmads13* Tos17 insertion mutant (cv. Dongjin) in a heterozygous state since homozygous mutants are female-sterile (Dreni *et al.*, 2007). Segregating progenies of *Osmads13* heterozygous plants were genotyped by duplex PCR, and only wild-type and homozygous mutants were analysed. The Rice Functional Genomic Express Database (<http://signal.salk.edu/cgi-bin/RiceGE>) was searched for mutations in candidate genes, and T-DNA insertion lines were obtained from Postech. The primers used for genotyping are listed in [Supplementary Table S1](#) at *JXB* online.

We also used T-DNA insertional mutants of the Postech collection in the Dongjin background, specifically PFG_3A-13182.L (insertion in *ZOS3-19*), PFG_1B-24315.L (insertion in *OsHLLH10*), and PFG_3A-00989.R (insertion in *OsZHD8*).

Total RNA extraction and RNA-sequencing

Total RNA was extracted from pooled samples of 12–15 developing inflorescences (stages In6 and In7) using a PureLink RNA Mini Kit (ThermoFisher Scientific). Three biological replicates were collected for each of the two genotypes. RNA quality and quantity were assessed using gel electrophoresis, an Agilent BioAnalyzer, and a Nanodrop spectrophotometer (ThermoFisher Scientific). Following treatment with TURBO DNase I (ThermoFisher Scientific), samples of 4 µg of RNA were used to produce sequencing libraries using a TruSeq mRNA sample preparation kit (Illumina). Multiplex sequencing of poly(A) RNA samples (six samples per lane, single 50-bp reads for 20 million reads each sample) was carried out using an Illumina HiSeq 2000 platform at IGA Technology Services (Udine, Italy).

RNA-sequencing analysis

Gene expression levels were estimated using the standard Bowtie-TopHat-Cufflinks pipeline (Trapnell *et al.*, 2013) on the established gene model of

the Rice Genome Annotation Project (MSU 7.0 non TE release) (Kawahara *et al.*, 2013) without performing a *de novo* assembly of the transcriptome. Differential expression analyses were performed using DESeq (Bioconductor version, release 2.12), and only genes with a false discovery rate lower than 0.05 were considered. Following GO-slim annotation, enrichment tests were performed using the AgriGO analysis toolkit (Du *et al.*, 2010), with a custom background formed only by expressed genes (FRPKM \geq 1).

The raw sequencing data produced in this study have been deposited at the NCBI short read archive (SRA) under the accession PRJNA638800. Gene expression patterns of the inflorescences of the wild-type and the *OsMADS1* loss-of-function mutant were retrieved from the following NCBI GEO datasets: GSE62078, GSE62078, GSE62078, GSE62078, GSE62078, GSE62078, GSE62078. Venn diagrams of overlapping gene lists were generated with tools available at http://bioinformatics.psb.ugent.be/cgi-bin/liste/Venn/calculate_venn.html. For selected candidate genes, information on paralogous and orthologous genes were retrieved from <http://gramene.org/>, whilst transcription domains were inferred from <http://ricexpro.dna.affrc.go.jp>.

Sample collection and preparation for laser-assisted micro-dissection

Developing inflorescences were collected and fixed under vacuum with acetone for 15 min. This was replaced with fresh acetone, and the samples were left at 4 °C overnight. For infiltration, the acetone was replaced first with an acetone/xylene series and then by molten Paraplast Xtra (Sigma-Aldrich), which was changed every 2 h for 24 h at 54 °C. The embedded samples were stored at 4 °C. Frame slides (PET Membrane; Leica Microsystems) and stands for laser-assisted micro-dissection (LMD) were sterilized by irradiation with UV light for 30 min using a UV cross-linker (Stratalinker 1800, Stratagene).

Embedded samples were cut into 10-µm sections on a rotary microtome, and ribbons containing a few sections were stretched on the treated frame slides with methanol for a maximum of 30 min at 37 °C (under a chemical hood). The slides were then immersed twice in xylene (5 min each) to dissolve the paraffin, and air-dried for 5 min at room temperature. For each sample, 80–100 cuts were obtained using a LMD 6000 system (Leica) equipped with an Axiovert 200 Inverted Fluorescent Microscope (Zeiss). Membrane-bound cells were collected into 0.5-ml tube caps (low-bind; Eppendorf) and resuspended in extraction buffer (see below). After 30 min incubation at 42 °C, the samples were stored at –80 °C until further use.

RNA extraction from specific cell types and cDNA amplification

Total RNA was extracted from pooled samples of the specific cell types obtained by LMD using an Arcturus PicoPure RNA Isolation Kit (ThermoFisher Scientific) according to the manufacturer's instructions. Genomic DNA was removed using DNase I (Qiagen) on column during the RNA extraction procedure. The integrity of the extracted RNA samples was assessed using an RNA 6000 Pico Kit on a 2100 BioAnalyzer (both Agilent Technologies). The RNA integrity number of our samples ranged from 7.10–7.40, which is of acceptable quality for down-stream application (Takahashi *et al.*, 2013). Because of the low quantity of starting material, 50 ng of the total RNA extracted from the LMD materials was used to produce up to 5 µg of amplified cDNA using the Ovation PicoSL WTA System V2 (NuGEN) following the manufacturer's instructions.

Expression analysis

For standard reverse-transcription quantitative (RT-q)PCR, RNA samples were treated with DNaseI RNase-free and retro-transcribed using the ImProm system (Promega). cDNA samples were used in qPCR reactions using iQ SYBR Green SuperMix on a CFX96 Touch Real-Time System (Bio-Rad).

High-throughput qPCR was carried out using a Microfluidic Dynamic Array developed by the Fluidigm Corporation (Spungeon *et al.*, 2008). A fast-cycling protocol was used on a Fluidigm BioMark machine using EvaGreen (Bio-Rad) as the dye. The experiment was performed at the Genomics Platform of CRAG (Barcelona, Spain), following the workflow provided by the manufacturer. For each sample, three technical replicates were performed and data were normalized using *OsEF1* or *OsUBQ* as the internal standard. Three biological replicates were used to determine relative expression.

For each experiment, statistical significance was determined using unpaired Student's two-tailed *t*-tests, with a confidence interval of 95%. The primers used for standard and large-scale qPCR are listed in [Supplementary Table S2](#).

In situ hybridization was performed as previously described by [Dreni *et al.* \(2007\)](#).

Phenotypic analyses of transgenic lines

We generated transgenic plants expressing an OsMADS13-GFP fusion protein (see Results and [Supplementary Fig. S13](#)). Reproductive organs were dissected at anthesis from mature flowers of the wild-type and the transgenic lines, and were examined using an Axiophot D1 microscope fitted with an AxioCam MR camera (both Zeiss). Samples for histological analysis and whole-mount tissue clearing were prepared as previously described ([Dreni *et al.*, 2007, 2011](#)).

Longitudinal thin sections (5 μ m thick) of mature pistils from the wild-type and *dst* mutant, previously embedded in Technovit resin, were stained with 0.1% Toluidin Blue and mounted with a coverslip.

Developing ovaries were dissected from wild-type plants and transgenic lines carrying the OsMADS13-GFP fusion and images were taken under bright field and under UV light to observe alterations in stigma formation and to detect the GFP signal in the transgenic lines.

Analysis of putative regulatory sequences of differentially expressed genes

We searched for AGAMOUS-like binding sites (CC (A/T)₅₋₇ GG) in the loci of interest (3 kb upstream of the transcription start site, exons, introns, 5'- and 3'-UTRs) using the TRANSFAC website (<http://gene-regulation.com/pub/databases.html>). Based on previous findings, two criteria were followed: regulatory sequences must contain a maximum of one mismatch in the CG clamp or in the A/T core, and at least two CA_nG-boxes within 600 bp.

Direct binding of OsMADS13 to downstream genes

To generate the set of reporter vectors, different promoter regions of *DL*, *ZOS3-19/DST*, and *OsZHD8* were cloned as Sall-PstI fragments in a modified pGreenII 0800-LUC vector carrying *Pro35S::LUC* and *Pro35S::REN* as the internal control to estimate the proportion of transformed protoplasts. Protoplasts were isolated from rice calli by digesting the cell wall with macerozyme R-10 and cellulase (Yakult Pharmaceuticals). Different combinations of the *Pro35S::OsMADS13* effector and the reporter vectors were co-transfected using PEG. After 18 h incubation in darkness at 24 °C, the transformed protoplasts were pelleted and resuspended in homogenization buffer for RNA extraction. The transactivation activity of OsMADS13 was assessed using RT-qPCR by calculating the relative ratio of mRNA abundance of the *Luciferase* and *Renilla* reporter genes. Three biological replicates were performed. Statistical significance was determined using unpaired Student's two-tailed *t*-tests, with a confidence interval of 95%. The primers used for the transient assays are listed in [Supplementary Table S3](#).

Results

Transcriptome analysis of the Osmads13 mutant versus the wild-type during flower development

We grew wild-type and *Osmads13* mutant rice plants for 8 weeks under long days (LD) and then transferred them to short days (SD) to induce flowering. Under these conditions, floral transition took place within one week following the transfer, and the formation and differentiation of floral organs began in a basipetal manner 2 weeks after induction ([Itoh *et al.*, 2005](#)). Under our experimental conditions, the developing inflorescences were characterized by a gradient of floral organ formation, with early stages being at the bottom whilst late stages are at the top. Macroscopic differences between the wild-type and the *Osmads13* mutant became visible only once the floral organs were fully formed. While ovules develop in wild-type florets, ectopic carpels develop in place of ovules in *Osmads13* florets ([Dreni *et al.*, 2007](#)). We performed RNA-sequencing analysis using whole immature inflorescences to identify genes that were deregulated in the mutant.

Developing inflorescences (5–8 mm long) were harvested from plants 3 weeks after the transfer from LD to SD, total RNA was extracted, and poly(A)-selected libraries were sequenced. Reads were mapped to the reference genome of *Oryza sativa* subsp. *japonica* cv. Nipponbare and the transcriptional profiles of wild-type and *Osmads13* were compared. We identified a total of 811 differentially expressed genes (DEGs) ($P \leq 0.05$) in *Osmads13*. This number was reduced to 476 genes when the Benjamini–Hochberg technique for the control of the false discovery rate was applied (cut-off of 0.05; [Supplementary Data Set S1](#)). Annotation of these DEGs based on the GO-slim ontology suggested that 11 were related to transposable elements (TEs) and 80 encoded proteins with unknown function, leaving 376 DEGs with assigned functions ([Fig. 1A](#)). We then divided the latter group into the following functional categories: metabolism (31%), nucleic acid binding (26%), protein binding (17%), structural components (16%), and response to endogenous and exogenous stimuli (10%) ([Fig. 1B](#)).

Gene ontology (GO) enrichment analyses were conducted using the whole set of expressed genes as the background, and identified 'DNA binding' and 'transcription regulator activity' as the most over-represented ontologies in the molecular function class; conversely, the term 'catalytic activity' was under-represented ([Fig. 1C](#)). Interestingly, we observed a high enrichment of the term 'transcription factor activity' ([Supplementary Fig. S1A](#)), especially when only DEGs up-regulated in *Osmads13* were considered ([Supplementary Fig. S1B](#)). In contrast, categories related to 'protein binding' were over-represented in the group of genes down-regulated in *Osmads13* ([Supplementary Fig. S1C](#)).

For genes related to regulation of transcription, the most represented TF families were APETALA2 and zinc-finger

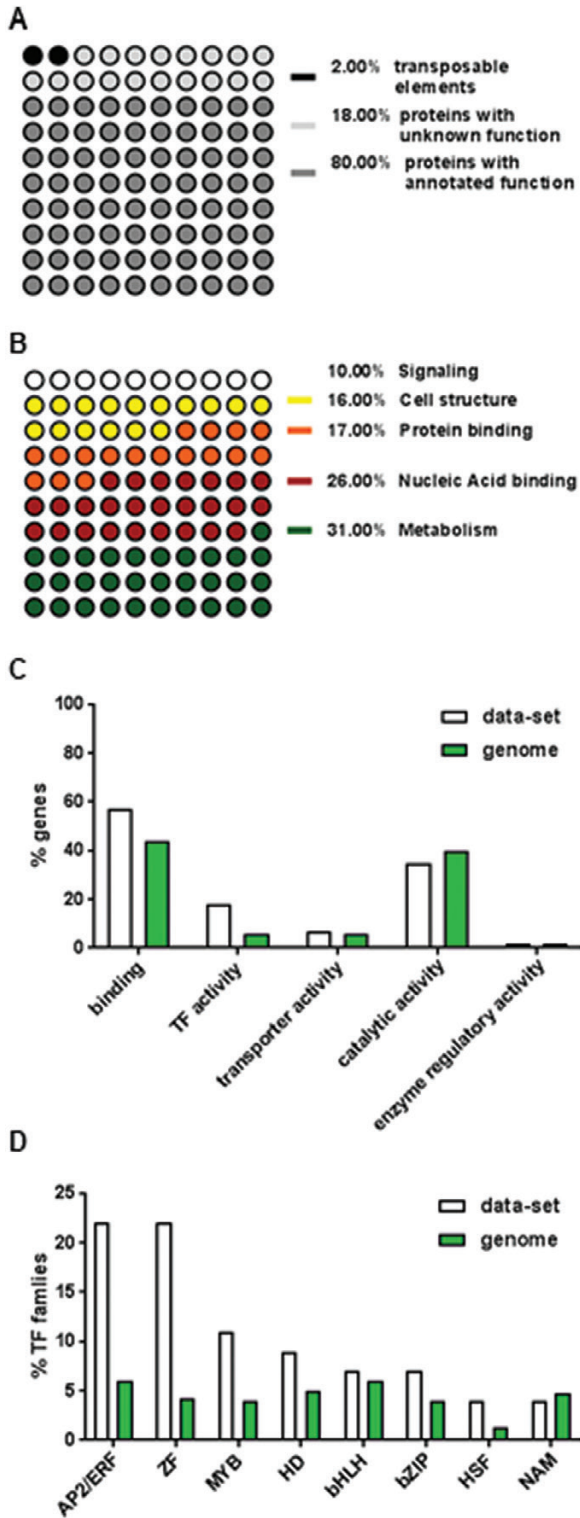


Fig. 1. GO annotation and classification of differentially expressed genes (DEGs) in the rice *Osmads13* mutant. (A) Dot-plot representing the classification of DEGs in *Osmads13* in sequences related to transposons and retrotransposons, expressed genes encoding proteins with unknown function, and genes encoding proteins with annotated functions, as indicated. The information was retrieved from the Database of Rice Transcription Factors (<http://plntfdb.bio.uni-potsdam.de/v3.0/index>.

(22%), followed by MYB (11%), homeo-domain (9%), basic helix-loop-helix and basic leucine zipper (7%), and heat-shock factors and no apical meristem (4%) (Fig. 1D). Surprisingly, 83% of the DEGs encoding DNA-binding proteins (67 of 81 genes) were up-regulated in *Osmads13* compared to 53% of the DEGs with an annotated function (199 of 375 genes), suggesting a de-repression of regulatory genes in the mutant inflorescences.

Known regulators of reproductive development are deregulated in Osmads13

OsMADS13 is activated slightly before ovule primordia (OPs) arise in the centre of the carpel, and it continues to be expressed throughout all stages of ovule development (Lopez-Dee et al., 1999; Dreni et al., 2007). We used laser-assisted micro-dissection (LMD) followed by RT-qPCR to monitor changes in the expression of selected genes in specific cell types, such as FMs and OPs isolated from flowers of the wild-type and the *Osmads13* mutant (Supplementary Fig. S2).

The stages and quality of the LMD tissues were assessed by monitoring the relative expression levels of the ovule identity gene *OsMADS13*, together with known genes involved in carpel development. As expected, *OsMADS13* transcripts were almost undetectable in the mutant plants (Fig. 2A). In contrast, *DROOPING LEAF (DL)*, a gene normally expressed in carpel tissue (Yamaguchi et al., 2004), was up-regulated in the *Osmads13* mutant (Fig. 2B). This is consistent with previous analyses based on *in situ* hybridization, showing ectopic transcription of *DL* in carpel-like organs of homeotic mutants (Dreni et al., 2007; Li et al., 2011). In our study, we found a 10-fold increase in *DL* expression in *Osmads13* at the early stages of flower formation, specifically in the cell types that were committed to differentiate into the ectopic

[php?sp_id=OSAJ](#)). (B) Dot-plot representing the annotation of DEGs in functional categories for components of metabolic pathways; proteins able to bind DNA, RNA, and chromatin; factors able to bind proteins (chaperons, protein modifiers, and regulatory enzymes); cell structure components (cell wall and membrane, cytoskeleton) together with proteins involved in the cell cycle (yellow); and signaling factors involved in the response to endogenous and exogenous stimuli. The percentages in each category are indicated. (C) GO analysis for molecular function of DEGs in *Osmads13* showing over-representation of the categories ‘binding’ and ‘transcription regulator activity’, and under-representation of the category ‘catalytic activity’. The information comes from Supplementary Data Set S1 and the Rice Genome Annotation Project (‘genome’; MSU 7.0 non TE release) (Kawahara et al., 2013). (D) The percentage of genes encoding single families of transcription factors in Supplementary Data Set S1 (81 out of 464 differentially expressed genes in *Osmads13* mutant encode TFs) and in the rice genome (2384 out of 39045 total genes in the rice genome encode TFs). AP2/ERF, APETALA2; ZF, zinc-finger; HD, homeo-domain; bHLH, basic helix-loop-helix; bZIP, basic leucine zipper; HSF, heat-shock factor; and NAM, no apical meristem. The remaining 14% are single members of other families. The information was retrieved from the Database of Rice Transcription Factors (2384 genes) and the Rice Genome Annotation Project (39045 genes).

carpels that replace the ovule in the mutant. We also observed increased levels of the AG subfamily genes *OsMADS3* (Fig. 2C) and *OsMADS58* (Fig. 2D), which are involved in carpel development. Conversely, we found decreased mRNA levels for the *LEAFY*-like gene *ABERRANT PANICLE ORGANIZATION 2* (*APO2*) and the *ARGONAUTE*-like (*AGO*) gene *MEIOSIS ARRESTED AT LEPTOTENE1* (*OsMEL1*) (Fig. 2E), which both encode factors involved in ovule and germ cell development (Nonomura *et al.*, 2007; Ikeda-Kawakatsu *et al.*, 2012). Taken together, these results supported the hypothesis that *OsMADS13* in OPs might directly or indirectly repress carpel identity genes (*DL*, *OsMADS3*, and *OsMADS58*) and activate genes involved in ovule development (*APO2* and *OsMEL1*). This is also consistent with the observed phenotype of the *Osmads13* mutant.

It was notable that *OsFD1/OsbZIP77* and *OsSPL14*, two regulatory genes with known roles in the control of meristematic activity during inflorescence development, continued to be expressed during flower development and were up-regulated in *Osmads13* primordia as compared to the wild-type (Supplementary Fig. S3). *OsFD1/OsbZIP77* is involved in the transition from a vegetative to a reproductive meristem (Taoka *et al.*, 2011), while *OsSPL14* determines the formation of primary and secondary branches of the inflorescence meristems (Jiao *et al.*, 2010; Miura *et al.*, 2010). The regulatory activity of *OsMADS13* therefore seems to extend to the repression of genes that are otherwise expressed throughout the reproductive phase.

Candidate genes expressed in reproductive tissues are deregulated in *Osmads13*

We used RT-qPCR to perform an additional validation of the RNA-seq results on a selection of DEGs without previously known functions in gynoecium development. Among the genes down-regulated in the mutant, we chose *OsbZIP52* (also known as *Rice Seed bZIP5*, *RBZ5*) due to its high expression after fertilization according to the RiceXPro database (Supplementary Fig. S4). We also analysed the expression of two loci (*LOC_Os02g13800* and *LOC_Os09g35790*) encoding heat-stress transcription factors (HSFs), and one locus (*LOC_Os01g08860*) encoding a heat-shock protein (HSP-like20). This choice was based on the evidence that chaperone activity was over-represented in the group of down-regulated genes in the *Osmads13* mutant (Supplementary Fig. S1C). We confirmed decreased transcript levels for these four genes in the inflorescences of *Osmads13* (Fig. 3A); however, only *HSP-like20* was also down-regulated in OPs in *Osmads13* (Fig. 3B).

Among the genes up-regulated in the mutant, we focused our analysis on interesting candidates belonging to the basic helix-loop-helix (bHLH) superfamily. This broad group of transcription regulators are involved in different developmental processes in numerous eukaryotic organisms (Massari and Murre, 2000). The first candidate gene, *LOC_Os04g23550* (*OsbHLH6*), belongs to a cluster of *bHLH* genes that includes

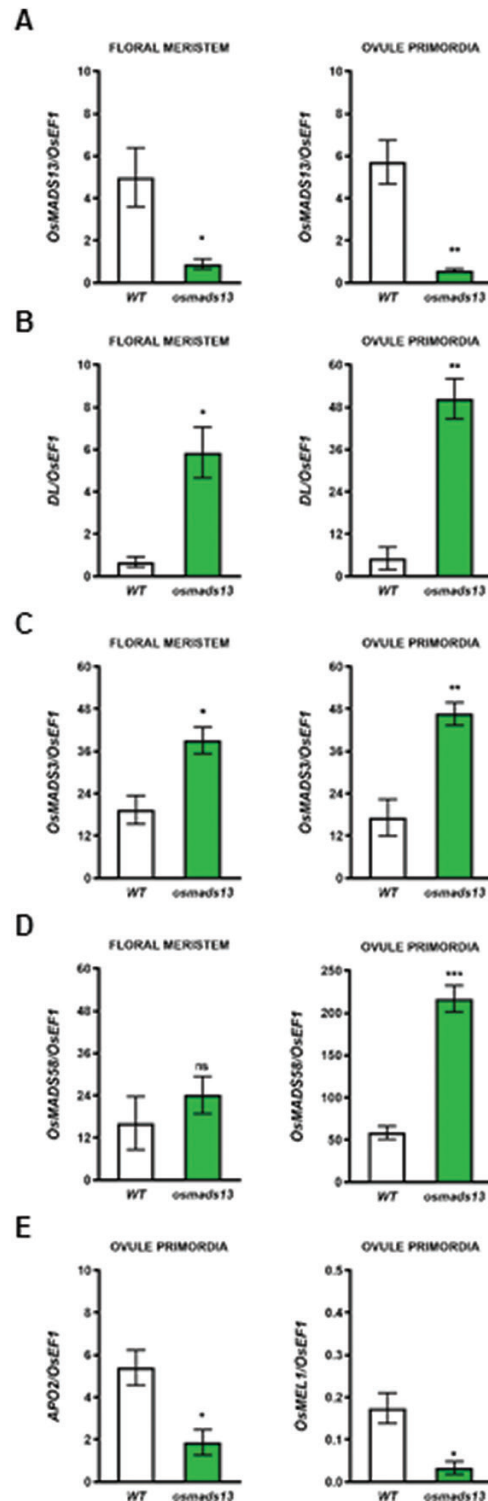


Fig. 2. Expression of known regulators of gynoecium development in wild-type (WT) rice and the *Osmads13* mutant. Relative expression in the floral meristem and ovule primordia of (A) the ovule identity gene *OsMADS13*, (B) the carpel marker gene *DL*, (C) *OsMADS3*, and (D) *OsMADS58*. (E) Relative expression in ovule primordia of *APO2* and *OsMEL1*. Expression levels were determined using RT-qPCR with *Rice Elongation Factor 1* as the internal standard. Data are means (\pm SD) of three biological replicates. Significant differences between means were determined using Student's *t*-test: * $P < 0.033$; ** $P < 0.002$; *** $P < 0.001$; ns, not significant.

UNDEVELOPED TAPETUM (*UDT1*; Jung *et al.*, 2005) and *TAPETUM DEGENERATION RETARDATION* (*TDR*; Li *et al.*, 2006), two important regulators of pollen development (Supplementary Fig. S5A). In addition to anthers, *OsBHLH6* also seemed to be expressed in reproductive meristems (Supplementary Fig. S5B), developing carpels, and ovaries after pollination (Supplementary Fig. S5C). This gene has two putative splicing isoforms that differ in length, with the shorter one lacking the basic domain necessary for DNA binding (i.e. the first two exons and the second intron of the longer variant are included in the 5'-UTR of the shorter variant). Specific primers were designed to discriminate between the two alternatively spliced transcripts (Fig. 3C). Expression analysis using primers amplifying the 3'-end of *OsBHLH6* (common for both variants) revealed strong up-regulation of this gene in the inflorescence and OPs in the *Osmads13* mutant (Fig. 3D). In contrast, the use of primers specific to *OsBHLH6.2* revealed an almost complete absence of the shorter transcript in both the tissues examined (Fig. 3E), indicating little or no contribution by the short-splicing variant to the mRNA abundance for this locus.

A second candidate gene, *LOC_Os01g50940* (*OsBHLH10*), was found to cluster together with *MYC2-like* genes (Supplementary Fig. S6; Fernández-Calvo *et al.*, 2011), and specifically with *JASMONATE ASSOCIATED MYC2-like* (*JAMs*) loci, which encode transcriptional repressors involved in the JA response (Sasaki-Sekimoto *et al.*, 2013) and in male fertility (Nakata and Ohme-Takagi, 2013). The expression of this gene was almost undetectable in FMs of the wild-type and mutant but it was strongly up-regulated in inflorescences and OPs of the *Osmads13* mutant (Fig. 3F).

The final candidate gene, *LOC_Os09g24490* (*OsBHLH39*), was selected because it shares common features with *TARGET of MONOPTEROS 5* (*TMO5*) and *TMO5-like*, which have been described as important regulators of the formation of lateral organs such as roots and ovules in Arabidopsis (Moreno-Risueño *et al.*, 2010; Galbiati *et al.*, 2013); Supplementary Fig. S7). *OsBHLH39* was highly expressed during reproductive development and was up-regulated in both the inflorescence and OPs in the *Osmads13* mutant (Fig. 3G).

Overlapping transcriptomes of D- and E-class loss-of-function mutants

In Arabidopsis, SEP and AG proteins form dimers to control the identity of carpels and ovules in the innermost whorl of developing flowers (Honma and Goto, 2001; Favaro *et al.*, 2003). Recent analyses have also shown that SEP3 and AG can form tetramers to control a subset of target genes involved in FM determinacy (Hugouvieux *et al.*, 2018). Moreover, previous molecular and genetic studies of floral homeotic factors in rice have indicated a network of complex molecular interactions between members of these two subfamilies (Cui *et al.*, 2010; Hu *et al.*, 2015). To gain deeper insights into the possible

interplay between D- and E-class factors during gynoecium development, we compared the list of DEGs in the immature inflorescences of *Osmads13* with previously published collections of genes deregulated in an *OsMADS1* knock-down (*OsMADS1-RNAi*) and knock-out (*Osmads1-z*) plants (Khanday *et al.*, 2013; Hu *et al.*, 2015). Interestingly, half of the DEGs in *Osmads13* were also deregulated in *OsMADS1-RNAi* and/or in *Osmads1-z* inflorescences (Supplementary Dataset S2). A total of 67% of genes up-regulated in *Osmads13* (131 of 197, group I) were down-regulated in the *Osmads1* loss-of-function mutants (Fig. 4A), and 33% of genes down-regulated in *Osmads13* (59 of 177, group II) were up-regulated in the *Osmads1* loss-of-function mutants (Fig. 4B). GO analysis for biological processes of group I revealed significant enrichment for the terms 'response to endogenous stimulus' and 'signal transduction' (Fig. 4C), consistent with the functions of *OsMADS1* and *OsMADS13* in regulating flower development. Similar analysis for group II revealed enrichment of the terms 'photosynthesis' and 'generation of precursors and metabolite' (Fig. 4D), which was probably due to the conversion of all floral organs into green photosynthetic tissues (glume-like organs) in the *Osmads1* loss-of-function mutants. Hence, the comparison of transcriptomic changes in these floral homeotic mutants suggested that *OsMADS1* and *OsMADS13* might act antagonistically on a common set of genes at early stages of flower development.

Since the ontology term 'transcription factor activity' was over-represented in our GO enrichment analysis (Supplementary Fig. S8A), putative downstream targets genes encoding for transcriptional regulators were considered for further analyses. To identify likely direct targets, we limited these analyses only to genes with two or more *CArG* boxes in their putative regulatory regions (3-kb promoter upstream of the transcription start site), the untranslated regions (5'- and 3'-UTRs), and the gene body (introns and exons). Interestingly, 14% of the DEGs in *Osmads13* contained MADS consensus binding sites that appeared to be bound by *OsMADS1* (Khanday *et al.*, 2016; Supplementary Dataset S3, Supplementary Fig. S8B), including *APO2*, *OsSPL14*, and *bZIP52*.

Validation of the dataset using zinc-finger transcription factor mutants

To investigate whether our data could be used to identify genes acting downstream of *OsMADS13* and thereby allow us to gain new insights into the regulatory mechanisms underlying gynoecium development in rice, we selected several T-DNA insertion mutants for a preliminary phenotypic analysis. Although the expression profiles of the chosen *OsBHLH* genes suggested a possible role in carpel development, examination of the mutant lines did not reveal any evident phenotypic defects characterized by an insertion in the 5'-UTR of *OsBHLH10* (Supplementary Fig. S9A, B), probably

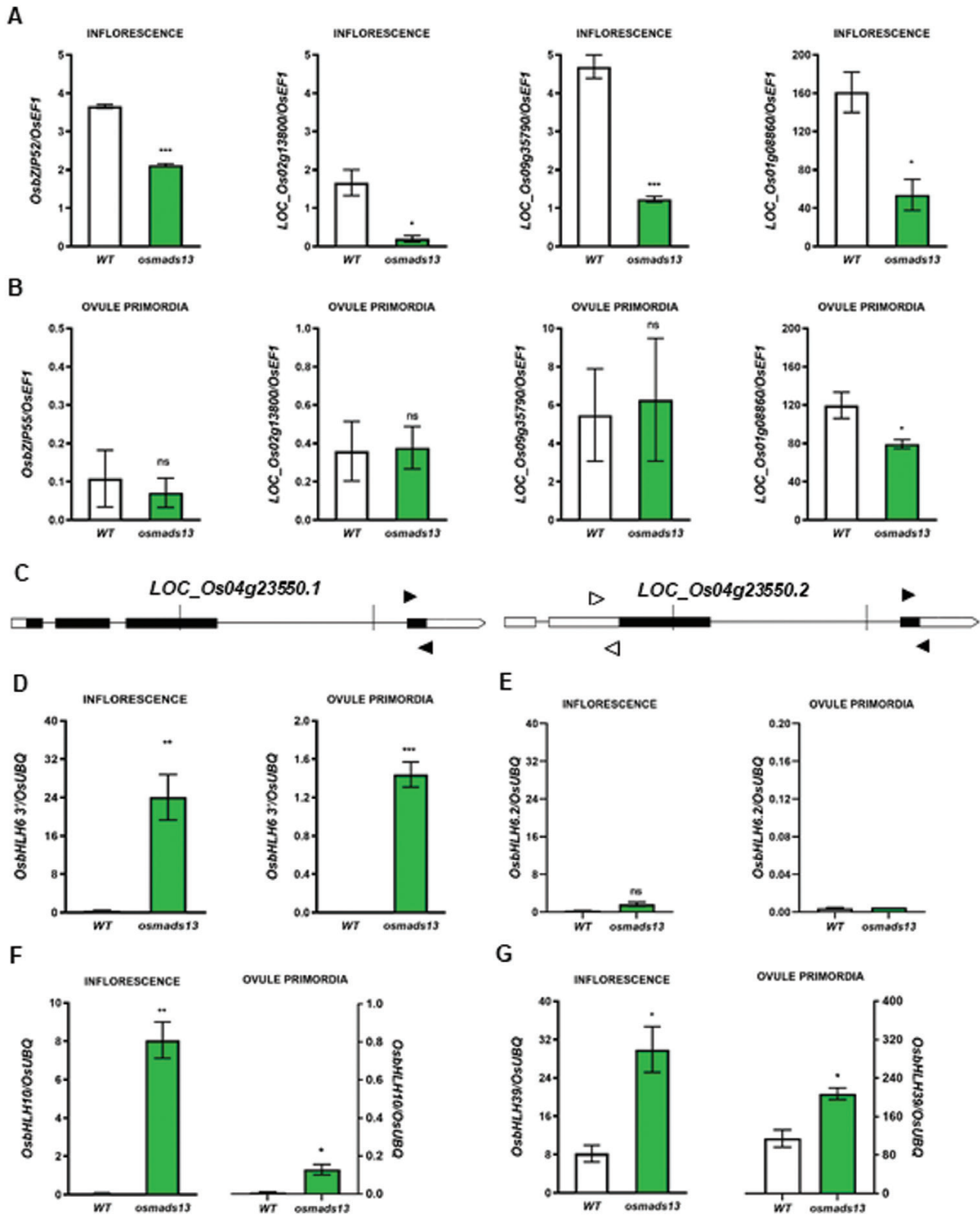


Fig. 3. Validation of RNA-seq in developing inflorescences and ovule primordia of wild-type rice and the *Osmads13* mutant. Relative expression levels of the *OsZIP52*, *HSF*, and *HSP* genes in (A) inflorescence and (B) ovule primordia of the wild-type (WT) and the mutant. (C) Schematic representation of the alternative transcripts of *OsHHLH6* and specific primers used to amplify the common 3'-end (black arrowheads, left) or the shorter transcript (white arrowheads, right). (D–G) Relative expression in inflorescences and ovule primordia of (D, E) the transcript variants of *OsHHLH6*, (F) *OsHHLH10*, and (G) *OsHHLH39*. Expression levels were determined using RT-qPCR with *OsEF1* and *OsUBQ* as the internal standards. Data are means (\pm SD) of three biological replicates. Significant differences between means were determined using Student's *t*-test: * $P < 0.033$; ** $P < 0.002$; *** $P < 0.001$; ns, not significant.

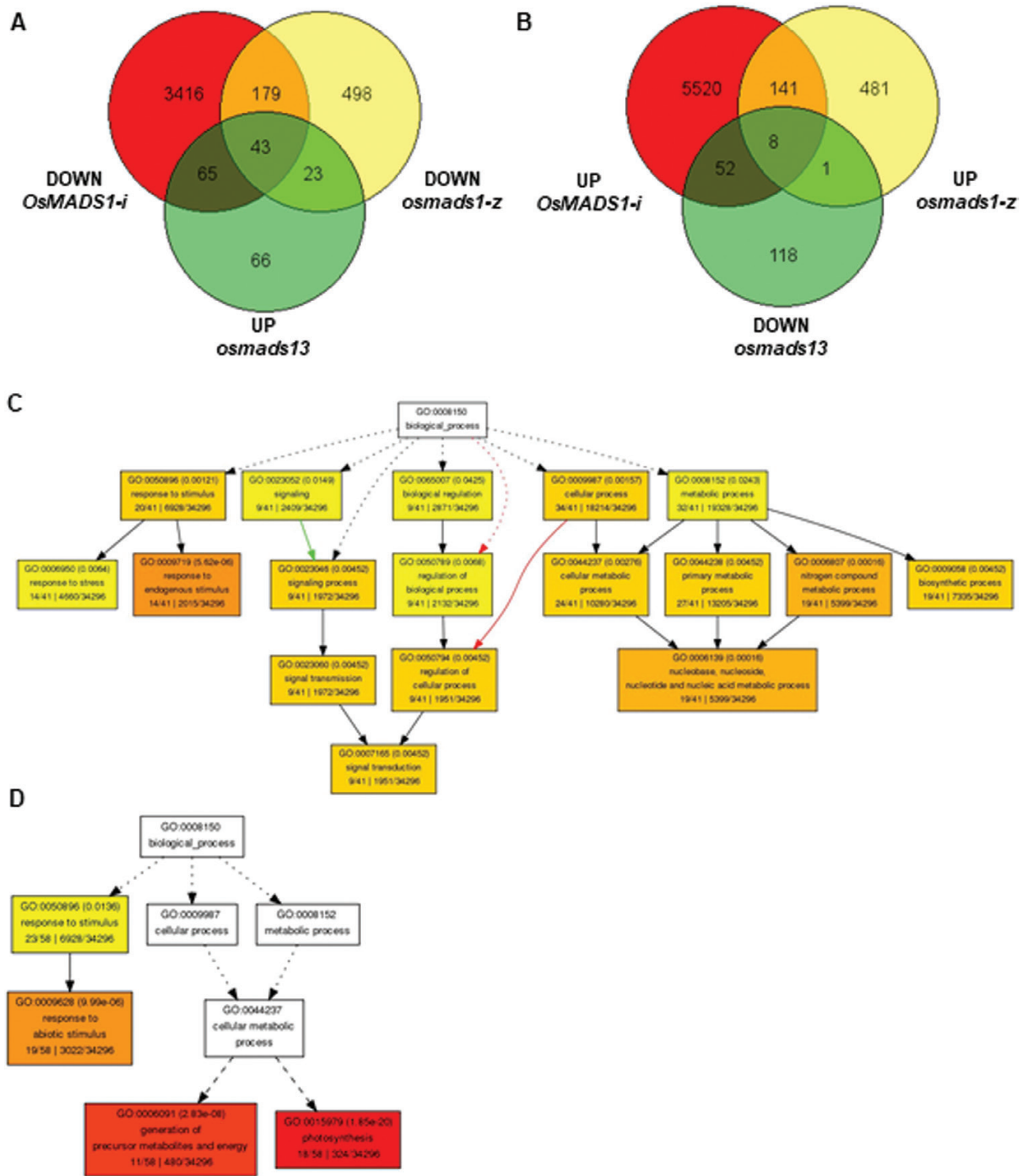


Fig. 4. Comparison of changes in the transcriptome of inflorescences of the rice *Osmads13* mutant and an *OsMADS1* loss-of-function mutant. (A, B) Venn diagrams showing common and specific differentially expressed genes in *Osmads13* (5–8-mm inflorescences, green), transgenic *OsMADS1*-RNAi (4–50-mm inflorescences, red; [Khanday et al., 2013](#)), and the loss-of-function mutant *Osmads1-z* (5–7-mm inflorescences, yellow; [Hu et al., 2015](#)). (C) Over-representation of the categories ‘response to endogenous stimulus’ and ‘signal transduction’ in group I (genes up-regulated in *Osmads13* and down-regulated in *Osmads1-z*). (D) Over-representation of the categories ‘photosynthesis’ and ‘generation of precursor metabolites and energy’ in group II (genes down-regulated in *Osmads13* and up-regulated in *Osmads1*). Singular enrichment analysis for molecular function was carried out using the Genome Annotation Project (MSU 7.0 non TE release) ([Kawahara et al., 2013](#)) transcript ID as the reference in AgriGO.

due to the small effect of T-DNA insertion on gene function. However, a similar T-DNA insertion in the 5'-UTR of *OsRAV11* (Supplementary Fig S9C) causes down-regulation and correlates with altered morphology of carpels and seeds in the homozygous mutant (Osnato *et al.*, 2020).

Insertion mutant lines for two candidate zinc-finger TFs also showed interesting phenotypes. The first, *LOC_Os03g57240* (*ZOS3-19*), is also known as *Drought and Salt Tolerance* (*DST*) and it is closely related to the domestication gene *PROSTRATE GROWTH 1* (*PROG1*; Tan *et al.*, 2008; Supplementary Fig. S10A). *DST* encodes a protein belonging to the Cys₂/Hys₂ (C₂H₂)-type zinc finger family of TFs comprising 113 members found only in *Oryza sativa* subsp. *japonica* (*ZOS*). Despite the high number of related genes in different monocotyledonous plants, this family has undergone significant gene loss events in dicotyledonous species. For instance, only the N-terminal region of *ZOS3-19/DST* has been found to exhibit remarkable similarities with a few Arabidopsis zinc-finger proteins (Supplementary Fig. S10B), such as GIS-like activators of trichome initiation (Gan *et al.*, 2006) and KNUCKLES (KNU; Payne *et al.*, 2004), JAGGED (JAG), and NUBBIN (NUB) (Dinneny *et al.*, 2006), which are required for reproductive organ development downstream of AG (Gómez-Mena *et al.*, 2005; Sun *et al.*, 2009).

According to the RiceXPro database, *ZOS3-19/DST* is widely expressed throughout plant development, with relatively high expression levels being observed in leaves and female reproductive tissues (Supplementary Fig. S10C). The *ZOS3-19/DST* transcript was strongly up-regulated in the *Osmads13* mutant (Fig. 5A, Supplementary Fig. S10D), and its *cis*-regulatory sequences contain several CArG boxes that are bound *in vivo* by OsMADS1 (Khanday *et al.*, 2016). Previous reports have indicated that *ZOS3-19/DST* plays several roles in rice development. For example, a mutant containing an amino acid substitution in the C₂H₂ domain displays enhanced tolerance to abiotic stresses due to its function in controlling stomatal functionality during the vegetative phase (Huang *et al.*, 2009). It is also notable that a different point mutation in the EAR motif—which is required for recruitment of co-repressors such as TOPLESS (TPL) and TPL-related proteins—is associated with increases in panicle branching and grain number as a consequence of increased cytokinin content in the reproductive meristems (Li *et al.*, 2013). To examine the effect of *ZOS3-19/DST* loss-of-function during gynoecium development, we studied a mutant harbouring a T-DNA insertion 109 bp downstream of the ATG codon, immediately before the sequence encoding the DNA-binding domain (Fig. 5B; Supplementary Fig. S10E). Morphological analysis of flowers of the *zos3-19/dst* insertion mutant showed alterations in the reproductive organs, such as shrunken stamens (normal filament, stunted anthers) and abnormal pistils (Fig. 5C). Detailed analyses by SEM revealed altered differentiation of the basal-apical tissues of the gynoecium, with slender ovaries, a reduced style, and shortened stigmas (Fig. 5D). In addition,

histological examination of mature flowers at anthesis showed that while the wild-type gynoecium developed a bottle-like ovary containing the female gametophyte, this tissue could not be found in the elongated ovary of the mutant gynoecium (Fig. 5E). Consequently, these mutants were completely sterile.

The other locus that we analysed, *OsZHD8*, encodes a putative Zinc-finger homeo-domain TF (Supplementary Fig. S11), which displays high levels of similarity with Arabidopsis proteins involved in vegetative and reproductive development, including *FLORAL TRANSITION AT THE MERISTEM2* (*FTM2*; Torti *et al.*, 2012). Significant up-regulation of *OsZHD8* was observed in the *Osmads13* mutant, especially in the OPs (Supplementary Fig. S12A–C). To explore its biological role, we studied a mutant characterized by a T-DNA insertion in the 3'-UTR of the gene (Supplementary Fig. S12D–F). Plants carrying this mutation in the homozygous state showed fertility defects that were probably caused by abnormal carpel development, specifically by alterations in the development of the stigma (Supplementary Fig. S12G). In addition to a reduced number of seeds, the *oszhd8* mutant also formed smaller panicles with fewer branches as compared to the wild-type (Supplementary Fig. S12H). These phenotypes were consistent with a possible regulatory role of *OsZHD8* in the control of meristematic activity during reproductive growth and in the correct development of reproductive organs.

In summary, our expression analyses and preliminary functional characterization of the insertion mutants allowed us to validate our datasets, and the results that we obtained have the potential to shed new light on the gene regulatory pathways acting downstream of OsMADS13, which is an important regulator of ovule identity.

Transactivation activity of OsMADS13 on candidate downstream genes

The DEGs identified in the *Osmads13* mutant could be directly or indirectly controlled by OsMADS13. Therefore, we first attempted to generate plants expressing an OsMADS13-GFP fusion protein for ChIP assays. However, the transgenic cassette *ProOsMADS13-OsMADS13(cds)-GFP* (the coding sequence of OsMADS13 under its native promoter) was not able to fully rescue the *Osmads13* mutant phenotype, as often a short tracheary element was observed instead of a functional megaspore mother cell (Supplementary Fig S13A). We also transformed the mutant with the full *OsMADS13* gene sequence including introns (Supplementary Fig S13B) and observed correct localization of the fusion protein (Supplementary Fig S13C); however, we were not able to overcome sterility problems (Supplementary Fig S13D). This could have been due to the absence of additional regulatory elements in the 3'-UTR or distal regions of the promoter, or alternatively due to the production of a GFP-tagged version of OsMADS13 that was not fully bioactive.

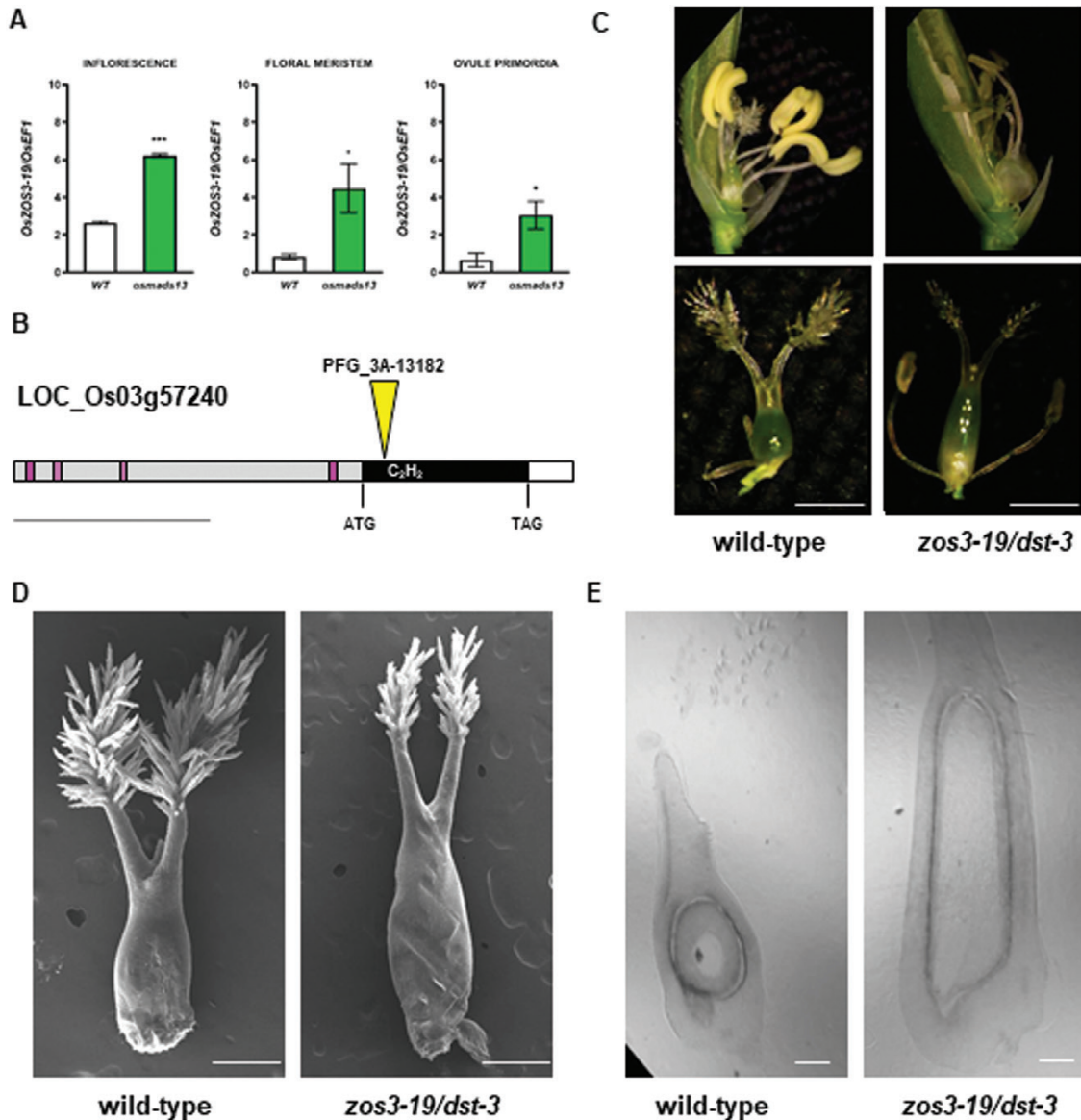


Fig. 5. Molecular and phenotypic analysis of rice *ZOS3-19/DST*. (A) Relative expression of *ZOS3-19/DST* in immature inflorescences, the floral meristem, and ovule primordia of the wild-type (WT) the *Osmads13* mutant. Expression levels were determined using RT-qPCR with *Rice Elongation Factor 1* as the internal standard. Data are means (\pm SD) of three biological replicates. Significant differences between means were determined using Student's *t*-test: * $P < 0.033$; *** $P < 0.001$. (B) Schematic representation of the *ZOS3-19* gene, with a T-DNA insertion (yellow triangle) 109 bp downstream of the ATG, just before the sequence encoding the zinc-finger domain (from 149 bp to 228 bp, corresponding to 49–76 aa). The 906-bp coding sequence is shown in black, the 3'-UTR is in white, the promoters are in grey, and the CArG boxes are in pink. The scale bar is 1 kb. (C) Representative images of floral organs (top) and carpels (bottom) of the WT and the *zos3-19/dst-3* mutant. Scale bars are 1 mm. (D) SEM images and (E) images of longitudinal thin sections (false-colored in grey) showing WT and *zos3-19/dst-3* gynoecia dissected from mature flowers at anthesis. Scale bars are 0.5 mm.

We therefore performed co-transformation assays based on a dual Renilla–Luciferase reporter system to test whether OsMADS13 was capable of direct binding to the regulatory regions containing CArG boxes of selected putative downstream genes, namely *DL*, *ZOS3-19/DST*, and *OsZHD8*. First, we analysed the genomic sequences of the putative targets and identified two regions for each candidate gene, one with and one without the MADS recognition site (schematic representations in Fig. 6, details in Supplementary Fig S14). Next, we

amplified and cloned the selected fragments upstream of the *LUC* coding sequence to generate the set of reporter vectors to be transiently co-expressed with the effector vector *Pro35S::OsMADS13* in rice protoplasts. Lastly, we studied the transactivation ability of OsMADS13 on these putative regulatory sequences by measuring the relative expression of the *LUC* and *REN* reporter genes in cell lysates. Although we could not find differences in co-transformation assays using sequences related to *OsZHD8* (Fig. 6A) and *ZOS3-19* (Fig. 6B), we

observed a significant decrease in LUC/REN relative transcript levels when OsMADS13 was co-transformed with a reporter vector carrying a fragment of *DL* intron IV containing multiple CArG boxes (Fig. 6C), suggesting that *DL*, as carpel-specific gene, might be directly targeted for repression by the ovule identity gene OsMADS13.

Discussion

Conservation and diversification of genetic pathways controlling gynoecium development in Arabidopsis and rice

The formation of various floral organs is coordinated by the actions and interactions of proteins encoded by members of the *MADS-box* gene family (reviewed by Jack, 2001; Immink *et al.*, 2010; O'Maoileidigh *et al.*, 2014). Interestingly, most of these factors are conserved among flowering plants even though the reproductive structures of dicotyledonous and monocotyledonous species display different features.

In the model dicot *Arabidopsis*, the floral meristem (FM) gives rise to four types of floral organs, and the formation of carpel primordia depletes FM activity (Lenhard *et al.*, 2001; Lohmann *et al.*, 2001). AG plays a crucial role in repressing stem cell proliferation and in promoting the differentiation of reproductive organs (Bowman *et al.*, 1989).

In rice, the C-class factors OsMADS3 and OsMADS58 redundantly control the development of reproductive organs as well as FM determinacy, similarly to *Arabidopsis* (Dreni *et al.*, 2011). However, the molecular mechanisms leading to the termination of the FM are still poorly understood, partly due to the absence of a functional counterpart of *WUS* in rice. OsMADS13 is highly similar to the *Arabidopsis* D-class factor *STK*, which not only controls ovule identity but also carpel and fruit development (Pinyopich *et al.*, 2003; Mizzotti *et al.*, 2014; Ezquer *et al.*, 2016; Herrera-Ubaldo *et al.*, 2019; Di Marzo *et al.*, 2020). Despite many commonalities, the mechanisms underlying ovule development in these two species are rather different. In *Arabidopsis*, the FM is completely consumed with the formation of the carpel, so that multiple ovule primordia (OPs) develop from placental tissues derived from the carpel margin meristem (Cucinotta *et al.*, 2014). By way of contrast, in rice a single ovule develops from the placental meristem, which derives directly from the inner part of the FM. This means that distinct from *Arabidopsis*, where *STK* does not necessarily have a meristem determinacy function, in rice OsMADS13 probably contributes to this function, as previously shown by analysis of the *Osmads13* single-mutant and by crossing the *Osmads13* mutant with the *Osmads3 Osmads58* double-mutant (Dreni *et al.*, 2007, 2011).

Similar sets of genes act downstream of AG and OsMADS13

In *Arabidopsis*, genome-wide approaches have shown that AG directly activates different regulatory factors, including

several *MADS-box* genes acting in reproductive growth and three closely related *ARGONAUTE* (*AGO*) genes encoding RNA-binding proteins (Ó'Maoileidigh *et al.*, 2013, 2018). In addition, AG and SEP proteins converge on the transcriptional regulation of *CRABSCLAW* (*CRC*), a gene encoding a YABBY TF that determines carpel development (Alvarez and Smyth, 1999). Indeed, *CRC* is a direct target of AG (Gómez-Mena *et al.*, 2005), and is ectopically expressed in carpelloid structures of higher-order mutants (Brambilla *et al.*, 2007).

In our study, GO enrichment analyses of DEGs revealed a significant enrichment in transcription regulatory activity in the *Osmads13* mutant (Fig. 1C, Supplementary Fig. 1B), in accordance with previous observations for the *ag* mutant (Ó'Maoileidigh *et al.*, 2013). Likewise, similar gene families seem to act downstream of OsMADS13 in the rice gynoecium. Indeed, we found up-regulation of the carpel identity genes *OsMADS3*, *OsMADS58* and *DL* (Fig. 2B–D), the rice ortholog of *CRC* (Yamaguchi *et al.*, 2004). Conversely, *OsMEL1*, an *AGO-like* gene essential for germ cell development, was down-regulated in *Osmads13* (Fig. 2E). Nevertheless, the interplay between floral homeotic proteins seems to be more complex in grasses, probably due to the diversification and neo-functionalization of SEP-like and AG-like factors. For example, OsMADS1 mediates the repression of inflorescence meristem identity genes (Khanday *et al.*, 2013) and promotes the early activation of genes involved in floral organ formation (Hu *et al.*, 2015). In addition, OsMADS1 controls FM termination together with OsMADS3 and OsMADS58, but functions on partially independent pathways from OsMADS13 (Hu *et al.*, 2015). Our comparative transcriptomic analysis suggests that OsMADS1 and OsMADS13 might control the same developmental pathways in an antagonistic manner.

Novel players may control the balance between meristem maintenance and gynoecium patterning

At the molecular level, the *Arabidopsis* AG floral homeotic protein controls the termination of FM activity by directly repressing *WUS* (Liu *et al.*, 2011) and activating the transcriptional repressor *KNU* (Sun *et al.*, 2009, 2014). *KNU* also regulates the proximo-distal pattern of gynoecium development since ectopic structures resembling stamens and carpels develop from the placenta of *knu* flowers (Payne *et al.*, 2004). Besides *KNU*, other C₂H₂ zinc finger TFs are known to act downstream of AG. Specifically, *JAG* and the closely related *NUB* redundantly control reproductive growth as their loss of function affects the development of microsporangia inside the anther and the formation of carpel walls (Dinneny *et al.*, 2006). Strikingly, in the *jag nub* double-mutant the ovules are exposed as valve tissues open in the apical region (Dinneny *et al.*, 2006).

Here, we report the preliminary characterization of ZOS3-19/DST, a rice protein that contains a C₂H₂-type DNA-binding domain similar to those of *KNU*, *JAG*, and *NUB* (Fig. 5, Supplementary Fig. 10). Despite its wide expression pattern

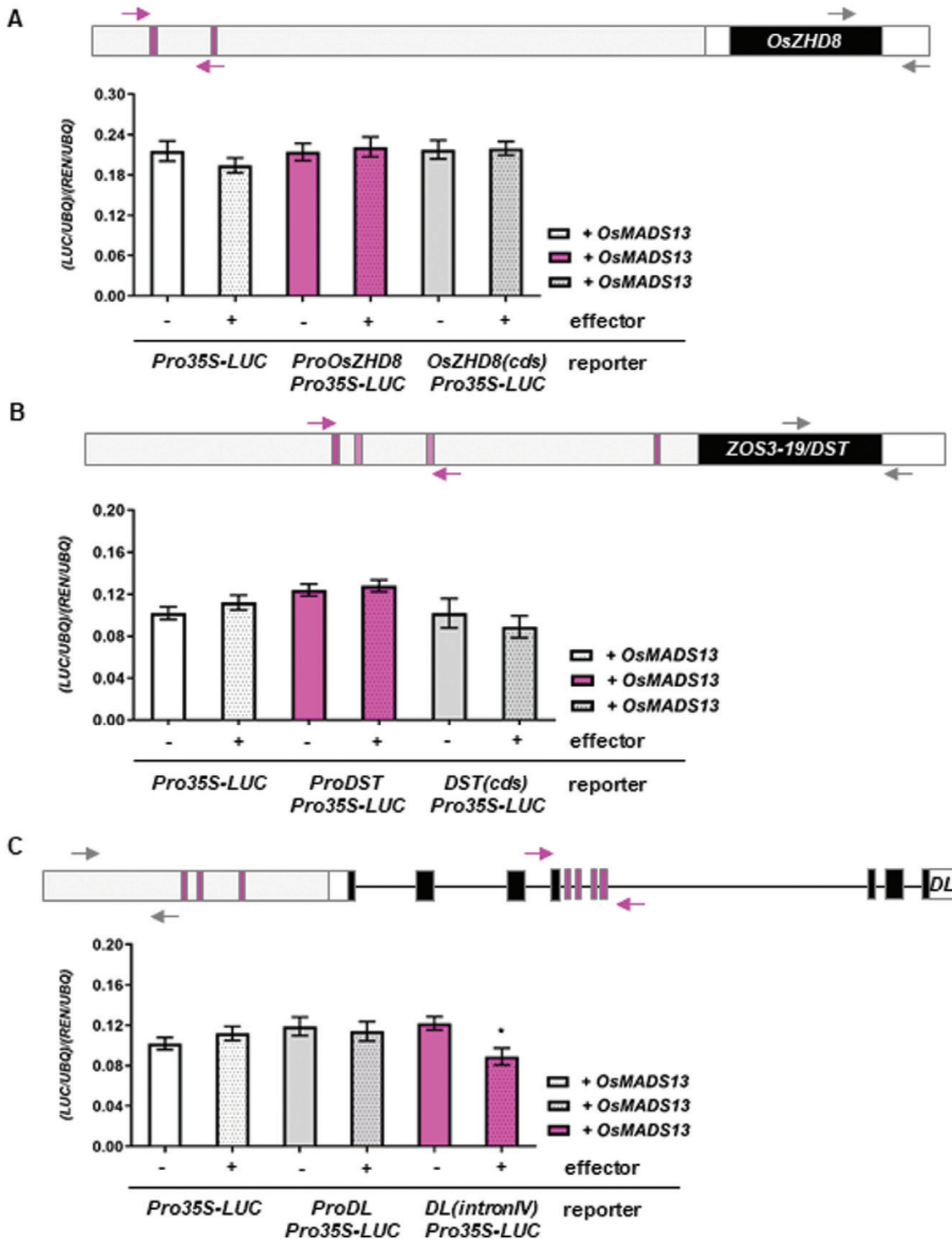


Fig. 6. Interactions between rice *OsMADS13* and putative targets. (A–C) Transactivation activity of *OsMADS13* in transiently transformed protoplasts, determined as the ratio of transcript levels of the *LUC* and *REN* reporter genes, relative to *UBQ*. The expression of *LUC* is driven by the putative regulatory sequences or the coding sequences of (A) *OsZHD8*, (B) *DST/ZOS3-19*, and (C) *DL*. Arrows represent primers used to amplify different fragments of putative downstream genes, either with (colored) or without (grey) MADS binding sites. Coding sequences are represented in black, UTRs are white, promoters are grey, and CARG and CARG-like sequences are pink.

throughout plant development (Supplementary Fig. 10C), a T-DNA insertion near the ATG codon caused macroscopic alterations in reproductive organs (Fig. 5C), with loss-of-function

correlating with wrinkled stamens and patterning defects of the carpel. Although morphological examination of the external structure of the latter seemed to suggest that the mutant pistil

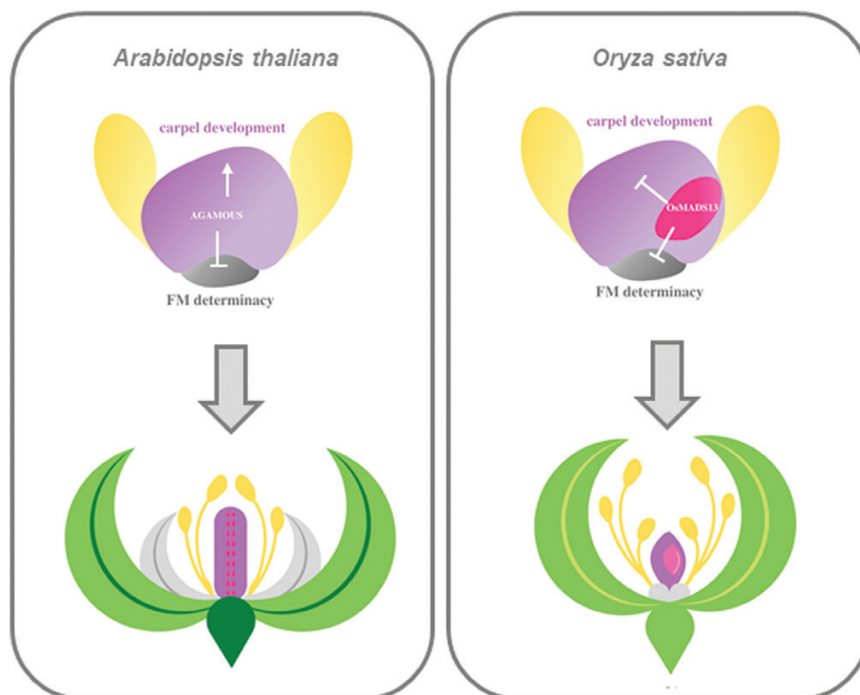


Fig. 7. A proposed model for the molecular mechanisms controlled by AGAMOUS (AG) in *Arabidopsis* and by OsMADS13 in rice. In *Arabidopsis*, AG controls the termination of the floral meristem (FM) by directly and indirectly repressing WUS, and activates genes involved in carpel development. In wild-type flowers, two fused carpels (in violet) containing ovule primordia (pink) develop in the innermost whorl. Stamens (yellow), petals (grey), and sepals (green) develop in the outer whorls. In rice, OsMADS13 might control the termination of FM indirectly by modulating hormone content and prevent the expression of genes involved in carpel formation in developing ovules. In wild-type flowers, the pistil (in violet) containing a single ovule primordium (pink) develops in the innermost whorl. Stamens (yellow), lodicules (grey), and glumes (green) develop in the outer whorls.

had been correctly differentiated (Fig 5D), abnormalities of the internal structure of the gynoecium indicated that the developmental program had stopped before the formation of the female gametophyte (Fig 5E). Hence, in flowers of the *zos3-19/dst* mutant, it is plausible that the pool of pluripotent cells of the FM is consumed during carpel development and the differentiation of the pistil along the basal–apical axis does not occur properly, leading to an elongated ovary and reduced style/stigmas (Fig. 5). Therefore, we propose a function for ZOS3-19/DST in controlling the balance between cell proliferation and differentiation. This could be achieved by modifying the hormonal content, in agreement with a previous report showing that ZOS3-19/DST regulates the expression of *OsCKX2*, which encodes an enzyme responsible for controlling the level of active cytokinins within developing reproductive tissues (Li *et al.*, 2013). Similarly, defects in gynoecium development and sterility problems were also observed in the *oszhd8* mutant (Supplementary Fig. 12), pointing to a role for this TF at different stages of flower formation. Both the *zos3-19/dst* and *oszhd8* mutants showed interesting female reproductive organ phenotypes (Fig 5C, Supplementary Fig. 12G) suggesting that our dataset has utility in identifying new candidate genes downstream of *OsMADS13*.

Direct binding of *OsMADS13* to putative target genes

Based on our expression analyses in reproductive tissues, we propose a role for *OsMADS13* as a master regulator of key

genes involved in the development of the gynoecium (Fig. 7). On one hand, ‘carpel genes’ must be switched off in those cells of the FM that would give origin to the OP in the wild-type and are de-repressed in the absence of functional *OsMADS13*. On the other hand, genes involved in gamete development should be activated in the OP during floral organ maturation before meiosis takes place.

Our transient transactivation assays in rice protoplasts indicated that *OsMADS13* could bind with at least the regulatory sequences containing CArG boxes in *DL* intron IV, and mediate the transcriptional repression of the reporter gene (Fig. 6C). Despite these promising results, further studies are required to confirm the direct binding of *OsMADS13* to other putative targets *in vivo*. In addition, further research using additional mutant alleles for candidate genes, potentially generated by CRISPR–Cas9 technology, will be needed to support these findings.

Supplementary data

The following supplementary data are available at *JXB* online.

Table S1. Primers used for PCR-based genotyping of the T-DNA insertion mutants.

Table S2. Primers used for gene expression analysis.

Table S3. Primers used for transactivation assays in rice protoplasts.

Fig. S1. GO enrichment analysis of statistically significant DEGs in the *Osmads13* mutant.

Fig. S2. Basipetal gradient of flower development along the rice inflorescence.

Fig. S3. Expression analyses of known regulators of rice reproductive development.

Fig. S4. *In silico* analysis of *OsbZIP52*.

Fig. S5. Phylogenomic and expression analysis of *OsbHLH6*.

Fig. S6. *In silico* analysis of *OsbHLH10*.

Fig. S7. *In silico* analysis of *OsbHLH39*.

Fig. S8. *In silico* identification of genes acting downstream of OsMADS1 and OsMADS13.

Fig. S9. T-DNA insertions in *OsbHLH10* and *OsRAV11*.

Fig. S10. Analysis of *ZOS3-19/DST*.

Fig. S11. *In silico* analysis of *OsZHD8*.

Fig. S12. Molecular and phenotypic analysis of *OsZHD8*.

Fig. S13. Generation and analysis of OsMADS13-GFP lines.

Fig. S14. *In silico* analysis of regulatory sequences of putative downstream targets of *DL*, *ZOS3-19/DST*, and *OsZHD8*.

Dataset S1. List of differentially expressed genes in *Osmads13* mutant.

Dataset S2. List of differentially expressed genes in *Osmads13* and *Osmads1* mutants.

Dataset S3. List of differentially expressed genes in *Osmads13* and bound by OsMADS1.

Acknowledgements

This work was supported by the FLOWER POWER project, a Lombardy Region (Italy) (Accordo di Collaborazione Scientifica e tecnologica) project for a bilateral collaboration between Milano-Barcelona. We thank Dr Pilar Fontanet (CRAG) for technical advice regarding the protoplast co-transformation assays, the Servei de Microscopia at the Universitat Autònoma de Barcelona (UAB) for help with SEM, and Mario Beretta and Valerio Parravicini for taking care of the rice plants.

Author contributions

MO performed most of the experiments, analysed the data, and prepared the graphics; EL conducted the expression analyses and co-transformation assays; AG conducted the *in situ* hybridization and laser micro-dissection; AP and LD performed the rice transformation and laser micro-dissection; MC and DH conducted the phylogenetic and RNA-sequencing data analyses; MO and MMK conceived the experimental design; and MO, MMK, and SP wrote the manuscript.

References

Agrawal GK, Abe K, Yamazaki M, Miyao A, Hirochika H. 2005. Conservation of the E-function for floral organ identity in rice revealed by the analysis of tissue culture-induced loss-of-function mutants of the *OsMADS1* gene. *Plant Molecular Biology* **59**, 125–135.

Alvarez J, Smyth DR. 1999. *CRABS CLAW* and *SPATULA*, two Arabidopsis genes that control carpel development in parallel with *AGAMOUS*. *Development* **126**, 2377–2386.

Balanza V, Roig-Villanova I, Di Marzo M, Masiero S, Colombo L. 2016. Seed abscission and fruit dehiscence required for seed dispersal rely on similar genetic networks. *Development* **143**, 3372–3381.

Bowman JL, Smyth DR, Meyerowitz EM. 1989. Genes directing flower development in Arabidopsis. *The Plant Cell* **1**, 37–52.

Bowman JL, Smyth DR, Meyerowitz EM. 2012. The ABC model of flower development: then and now. *Development* **139**, 4095–4098.

Brambilla V, Battaglia R, Colombo M, Masiero S, Bencivenga S, Kater MM, Colombo L. 2007. Genetic and molecular interactions between BELL1 and MADS box factors support ovule development in Arabidopsis. *The Plant Cell* **19**, 2544–2556.

Brand U, Fletcher JC, Hobe M, Meyerowitz EM, Simon R. 2000. Dependence of stem cell fate in Arabidopsis on a feedback loop regulated by CLV3 activity. *Science* **289**, 617–619.

Causier B, Castillo R, Xue Y, Schwarz-Sommer Z, Davies B. 2010. Tracing the evolution of the floral homeotic B- and C-function genes through genome synteny. *Molecular Biology and Evolution* **27**, 2651–2664.

Cucinotta M, Colombo L, Roig-Villanova I. 2014. Ovule development, a new model for lateral organ formation. *Frontiers in Plant Science* **5**, 117.

Cui R, Han J, Zhao S, Su K, Wu F, Du X, Xu Q, Chong K, Theissen G, Meng Z. 2010. Functional conservation and diversification of class E floral homeotic genes in rice (*Oryza sativa*). *The Plant Journal* **61**, 767–781.

Di Marzo M, Herrera-Ubaldo H, Caporali E, Novák O, Strnad M, Balanza V, Ezquer I, Mendes MA, de Folter S, Colombo L. 2020. SEEDSTICK controls Arabidopsis fruit size by regulating cytokinin levels and *FRUITFULL*. *Cell Reports* **30**, 2846–2857.e3.

Dinneny JR, Weigel D, Yanofsky MF. 2006. *NUBBIN* and *JAGGED* define stamen and carpel shape in Arabidopsis. *Development* **133**, 1645–1655.

Ditta G, Pinyopich A, Robles P, Pelaz S, Yanofsky MF. 2004. The *SEP4* gene of *Arabidopsis thaliana* functions in floral organ and meristem identity. *Current Biology* **14**, 1935–1940.

Dreni L, Jacchia S, Fornara F, Fornari M, Ouwerkerk PB, An G, Colombo L, Kater MM. 2007. The D-lineage MADS-box gene *OsMADS13* controls ovule identity in rice. *The Plant Journal* **52**, 690–699.

Dreni L, Pilatone A, Yun D, Erreni S, Pajoro A, Caporali E, Zhang D, Kater MM. 2011. Functional analysis of all AGAMOUS subfamily members in rice reveals their roles in reproductive organ identity determination and meristem determinacy. *The Plant Cell* **23**, 2850–2863.

Du Z, Zhou X, Ling Y, Zhang Z, Su Z. 2010. agriGO: A GO analysis toolkit for the agricultural community. *Nucleic Acids Research* **38**, W64–W70.

Egea-Cortines M, Saedler H, Sommer H. 1999. Ternary complex formation between the MADS-box proteins SQUAMOSA, DEFICIENS and GLOBOSA is involved in the control of floral architecture in *Antirrhinum majus*. *The EMBO Journal* **18**, 5370–5379.

Ezquer I, Mizzotti C, Nguema-Ona E, *et al.* 2016. The developmental regulator SEEDSTICK controls structural and mechanical properties of the Arabidopsis seed coat. *The Plant Cell* **28**, 2478–2492.

Favaro R, Pinyopich A, Battaglia R, Kooiker M, Borghi L, Ditta G, Yanofsky MF, Kater MM, Colombo L. 2003. MADS-box protein complexes control carpel and ovule development in Arabidopsis. *The Plant Cell* **15**, 2603–2611.

Fernández-Calvo P, Chini A, Fernández-Barbero G, *et al.* 2011. The Arabidopsis bHLH transcription factors MYC3 and MYC4 are targets of JAZ repressors and act additively with MYC2 in the activation of jasmonate responses. *The Plant Cell* **23**, 701–715.

Galbiati F, Sinha Roy D, Simonini S, *et al.* 2013. An integrative model of the control of ovule primordia formation. *The Plant Journal* **76**, 446–455.

Gan Y, Kumimoto R, Liu C, Ratcliffe O, Yu H, Broun P. 2006. GLABROUS INFLORESCENCE STEMS modulates the regulation by gibberellins of epidermal differentiation and shoot maturation in Arabidopsis. *The Plant Cell* **18**, 1383–1395.

Gómez-Mena C, de Folter S, Costa MM, Angenent GC, Sablowski R. 2005. Transcriptional program controlled by the floral homeotic gene *AGAMOUS* during early organogenesis. *Development* **132**, 429–438.

- Herrera-Ubaldo H, Lozano-Sotomayor P, Ezquer I, et al.** 2019. New roles of NO TRANSMITTING TRACT and SEEDSTICK during medial domain development in Arabidopsis fruits. *Development* **146**, dev172395.
- Honma T, Goto K.** 2001. Complexes of MADS-box proteins are sufficient to convert leaves into floral organs. *Nature* **409**, 525–529.
- Hu Y, Liang W, Yin C, et al.** 2015. Interactions of *OsMADS1* with floral homeotic genes in rice flower development. *Molecular Plant* **8**, 1366–1384.
- Huang XY, Chao DY, Gao JP, Zhu MZ, Shi M, Lin HX.** 2009. A previously unknown zinc finger protein, DST, regulates drought and salt tolerance in rice via stomatal aperture control. *Genes & Development* **23**, 1805–1817.
- Hugouvieux V, Silva CS, Jourdain A, Stigliani A, Charras Q, Conn V, Conn SJ, Carles CC, Parcy F, Zubieta C.** 2018. Tetramerization of MADS family transcription factors SEPALLATA3 and AGAMOUS is required for floral meristem determinacy in Arabidopsis. *Nucleic Acids Research* **46**, 4966–4977.
- Ikeda-Kawakatsu K, Maekawa M, Izawa T, Itoh J, Nagato Y.** 2012. *ABERRANT PANICLE ORGANIZATION 2/RFL*, the rice ortholog of Arabidopsis *LEAFY*, suppresses the transition from inflorescence meristem to floral meristem through interaction with *APO1*. *The Plant Journal* **69**, 168–180.
- Immink RGH, Kaufmann K, Angenent GC.** 2010. The 'ABC' of MADS domain protein behaviour and interactions. *Seminars in Cell & Developmental Biology* **21**, 87–93.
- Itoh JI, Nonomura KI, Ikeda K, Yamaki S, Inukai Y, Yamagishi H, Kitano H, Nagato Y.** 2005. Rice plant development: from zygote to spikelet. *Plant & Cell Physiology* **46**, 23–47.
- Jack T.** 2001. Plant development going MADS. *Plant Molecular Biology* **46**, 515–520.
- Jeon JS, Jang S, Lee S, et al.** 2000. *leafy hull sterile1* is a homeotic mutation in a rice MADS box gene affecting rice flower development. *The Plant Cell* **12**, 871–884.
- Jiao Y, Wang Y, Xue D, et al.** 2010. Regulation of *OsSPL14* by *OsmiR156* defines ideal plant architecture in rice. *Nature Genetics* **42**, 541–544.
- Jung KH, Han MJ, Lee YS, Kim YW, Hwang I, Kim MJ, Kim YK, Nahm BH, An G.** 2005. Rice *Undeveloped Tapetum1* is a major regulator of early tapetum development. *The Plant Cell* **17**, 2705–2722.
- Kaufmann K, Muiño JM, Jauregui R, Airolidi CA, Smaczniak C, Krajewski P, Angenent GC.** 2009. Target genes of the MADS transcription factor *sepallata3*: integration of developmental and hormonal pathways in the Arabidopsis flower. *PLoS Biology* **7**, e1000090.
- Kawahara Y, de la Bastide M, Hamilton JP, Kim YW, Hwang I, Kim MJ, Kim YK, Nahm BH, An G.** 2013. Improvement of the *Oryza sativa* Nipponbare reference genome using next generation sequence and optical map data. *Rice* **6**, 4.
- Khanday I, Das S, Chongloi GL, Bansal M, Grossniklaus U, Vijayraghavan U.** 2016. Genome-wide targets regulated by the *OsMADS1* transcription factor reveals its DNA recognition properties. *Plant Physiology* **172**, 372–388.
- Khanday I, Yadav SR, Vijayraghavan U.** 2013. Rice *LHS1/OsMADS1* controls floret meristem specification by coordinated regulation of transcription factors and hormone signaling pathways. *Plant Physiology* **161**, 1970–1983.
- Kubo T, Fujita M, Takahashi H, Nakazono M, Tsutsumi N, Kurata N.** 2013. Transcriptome analysis of developing ovules in rice isolated by laser microdissection. *Plant & Cell Physiology* **54**, 750–765.
- Laux T, Mayer KF, Berger J, Jürgens G.** 1996. The *WUSCHEL* gene is required for shoot and floral meristem integrity in Arabidopsis. *Development* **122**, 87–96.
- Lenhard M, Bohnert A, Jürgens G, Laux T.** 2001. Termination of stem cell maintenance in Arabidopsis floral meristems by interactions between *Wuschel* and *Agamous*. *Cell* **105**, 805–814.
- Li H, Liang W, Hu Y, Zhu L, Yin C, Xu J, Dreni L, Kater MM, Zhang D.** 2011. Rice *MADS6* interacts with the floral homeotic genes *SUPERWOMAN1*, *MADS3*, *MADS58*, *MADS13*, and *DROOPING LEAF* in specifying floral organ identities and meristem fate. *The Plant Cell* **23**, 2536–2552.
- Li N, Zhang DS, Liu HS, et al.** 2006. The rice *Tapetum Degeneration Retardation* gene is required for tapetum degradation and anther development. *The Plant Cell* **18**, 2999–3014.
- Li S, Zhao B, Yuan D, et al.** 2013. Rice zinc finger protein DST enhances grain production through controlling *Gn1a/OsCKX2* expression. *Proceedings of the National Academy of Sciences, USA* **110**, 3167–3172.
- Liljegren SJ, Ditta GS, Eshed Y, Savidge B, Bowmant JL, Yanofsky MF.** 2000. *SHATTERPROOF* MADS-box genes control dispersal in Arabidopsis. *Nature* **404**, 766–770.
- Liu X, Kim YJ, Müller R, Yumul RE, Liu C, Pan Y, Cao X, Goodrich J, Chen X.** 2011. *AGAMOUS* terminates floral stem cell maintenance in Arabidopsis by directly repressing *WUSCHEL* through recruitment of Polycomb Group proteins. *The Plant Cell* **23**, 3654–3670.
- Lohmann JU, Hong RL, Hobe M, Busch MA, Parcy F, Simon R, Weigel D.** 2001. A molecular link between stem cell regulation and floral patterning in Arabidopsis. *Cell* **105**, 793–803.
- Lopez-Dee ZP, Wittich P, Enrico Pè M, Rigola D, Del Buono I, Gorla MS, Kater MM, Colombo L.** 1999. *OsMADS13*, a novel rice MADS-box gene expressed during ovule development. *Developmental Genetics* **25**, 237–244.
- Malcomber ST, Kellogg EA.** 2004. Heterogeneous expression patterns and separate roles of the *SEPALLATA* gene *LEAFY HULL STERILE1* in grasses. *The Plant Cell* **16**, 1692–1706.
- Malcomber ST, Kellogg EA.** 2005. *SEPALLATA* gene diversification: brave new whorls. *Trends in Plant Science* **10**, 427–435.
- Massari ME, Murre C.** 2000. Helix-loop-helix proteins: regulators of transcription in eucaryotic organisms. *Molecular and Cellular Biology* **20**, 429–440.
- Matias-Hernandez L, Battaglia R, Galbiati F, Rubes M, Eichenberger C, Grossniklaus U, Kater MM, Colombo L.** 2010. *VERDANDI* is a direct target of the MADS domain ovule identity complex and affects embryo sac differentiation in Arabidopsis. *The Plant Cell* **22**, 1702–1715.
- Mendes MA, Guerra RF, Berns MC, Manzo C, Masiero S, Finzi L, Kater MM, Colombo L.** 2013. MADS domain transcription factors mediate short-range DNA looping that is essential for target gene expression in Arabidopsis. *The Plant Cell* **25**, 2560–2572.
- Miura K, Ikeda M, Matsubara A, Song XJ, Ito M, Asano K, Matsuoka M, Kitano H, Ashikari M.** 2010. *OsSPL14* promotes panicle branching and higher grain productivity in rice. *Nature Genetics* **42**, 545–549.
- Mizzotti C, Ezquer I, Paolo D, et al.** 2014. SEEDSTICK is a master regulator of development and metabolism in the Arabidopsis seed coat. *PLoS Genetics* **10**, e1004856.
- Moreno-Risueno MA, Van Norman JM, Moreno A, Zhang J, Ahnert SE, Benfey PN.** 2010. Oscillating gene expression determines competence for periodic Arabidopsis root branching. *Science* **329**, 1306–1311.
- Nakata M, Ohme-Takagi M.** 2013. Two bHLH-type transcription factors, JA-ASSOCIATED MYC2-LIKE2 and JAM3, are transcriptional repressors and affect male fertility. *Plant Signaling & Behavior* **8**, e26473.
- Nonomura K, Morohoshi A, Nakano M, Eiguchi M, Miyao A, Hirochika H, Kurata N.** 2007. A germ cell specific gene of the *ARGONAUTE* family is essential for the progression of premeiotic mitosis and meiosis during sporogenesis in rice. *The Plant Cell* **19**, 2583–2594.
- Ó'Maoiléidigh DS, Stewart D, Zheng B, Coupland G, Wellmer F.** 2018. Floral homeotic proteins modulate the genetic program for leaf development to suppress trichome formation in flowers. *Development* **145**, dev157784.
- O'Maoileidigh DS, Graciet E, Wellmer F.** 2014. Genetic control of Arabidopsis flower development. In: Fornara F, ed. *Advances in botanical research*, Vol. **72**. Academic Press, 159–190.
- Ó'Maoiléidigh DS, Wuest SE, Rae L, et al.** 2013. Control of reproductive floral organ identity specification in Arabidopsis by the C function regulator *AGAMOUS*. *The Plant Cell* **25**, 2482–2503.

- Osnato M, Matias-Hernandez L, Aguilar-Jaramillo AE, Kater MM, Pelaz S.** 2020. Genes of the *RAV* family control heading date and carpel development in rice. *Plant Physiology* **183**, 1663–1680.
- Payne T, Johnson SD, Koltunow AM.** 2004. *KNUCKLES (KNU)* encodes a C2H2 zinc-finger protein that regulates development of basal pattern elements of the Arabidopsis gynoecium. *Development* **131**, 3737–3749.
- Pelaz S, Ditta GS, Baumann E, Wisman E, Yanofsky MF.** 2000. B and C floral organ identity functions require *SEPALLATA* MADS-box genes. *Nature* **405**, 200–203.
- Pinyopich A, Ditta GS, Savidge B, Liljegren SJ, Baumann E, Wisman E, Yanofsky MF.** 2003. Assessing the redundancy of MADS-box genes during carpel and ovule development. *Nature* **424**, 85–88.
- Prasad K, Parameswaran S, Vijayraghavan U.** 2005. OsMADS1, a rice MADS-box factor, controls differentiation of specific cell types in the lemma and palea and is an early-acting regulator of inner floral organs. *The Plant Journal* **43**, 915–928.
- Prasad K, Sriram P, Kumar CS, Kushalappa K, Vijayraghavan U.** 2001. Ectopic expression of rice *OsMADS1* reveals a role in specifying the lemma and palea, grass floral organs analogous to sepals. *Development Genes and Evolution* **211**, 281–290.
- Sasaki-Sekimoto Y, Jikumaru Y, Obayashi T, Saito H, Masuda S, Kamiya Y, Ohta H, Shirasu K.** 2013. Basic helix-loop-helix transcription factors JASMONATE-ASSOCIATED MYC2-LIKE1 (JAM1), JAM2, and JAM3 are negative regulators of jasmonate responses in Arabidopsis. *Plant Physiology* **163**, 291–304.
- Schoof H, Lenhard M, Haecker A, Mayer KF, Jürgens G, Laux T.** 2000. The stem cell population of Arabidopsis shoot meristems is maintained by a regulatory loop between the *CLAVATA* and *WUSCHEL* genes. *Cell* **100**, 635–644.
- Spurgeon SL, Jones RC, Ramakrishnan R.** 2008. High throughput gene expression measurement with real time PCR in a microfluidic dynamic array. *PLoS One* **3**, e1662.
- Sun B, Looi LS, Guo S, He Z, Gan ES, Huang J, Xu Y, Wee WY, Ito T.** 2014. Timing mechanism dependent on cell division is invoked by Polycomb eviction in plant stem cells. *Science* **343**, 1248559.
- Sun B, Xu Y, Ng KH, Ito T.** 2009. A timing mechanism for stem cell maintenance and differentiation in the Arabidopsis floral meristem. *Genes & Development* **23**, 1791–1804.
- Takahashi J, Takatsu A, Iwahashi H.** 2013. Evaluation for integrity of extracted RNA by reference material of RNA. *Journal of Medical Diagnostic Methods* **2**, 128.
- Tan L, Li X, Liu F, et al.** 2008. Control of a key transition from prostrate to erect growth in rice domestication. *Nature Genetics* **40**, 1360–1364.
- Tang X, Zhang ZY, Zhang WJ, Zhao XM, Li X, Zhang D, Liu QQ, Tang WH.** 2010. Global gene profiling of laser-captured pollen mother cells indicates molecular pathways and gene subfamilies involved in rice meiosis. *Plant Physiology* **154**, 1855–1870.
- Taoka K, Ohki I, Tsuji H, et al.** 2011. 14-3-3 proteins act as intracellular receptors for rice Hd3a florigen. *Nature* **476**, 332–335.
- Theissen G, Melzer R.** 2007. Molecular mechanisms underlying origin and diversification of the angiosperm flower. *Annals of Botany* **100**, 603–619.
- Theissen G, Saedler H.** 2001. Floral quartets. *Nature* **409**, 469–471.
- Torti S, Fornara F, Vincent C, Andrés F, Nordström K, Göbel U, Knoll D, Schoof H, Coupland G.** 2012. Analysis of the Arabidopsis shoot meristem transcriptome during floral transition identifies distinct regulatory patterns and a leucine-rich repeat protein that promotes flowering. *The Plant Cell* **24**, 444–462.
- Trapnell C, Hendrickson DG, Sauvageau M, Goff L, Rinn JL, Pachter L.** 2013. Differential analysis of gene regulation at transcript resolution with RNA-seq. *Nature Biotechnology* **31**, 46–53.
- Yamaguchi N, Huang J, Xu Y, Tanoi K, Ito T.** 2017. Fine-tuning of auxin homeostasis governs the transition from floral stem cell maintenance to gynoecium formation. *Nature Communications* **8**, 1125.
- Yamaguchi T, Lee DY, Miyao A, Hirochika H, An G, Hirano HY.** 2006. Functional diversification of the two C-class MADS box genes *OSMADS3* and *OSMADS58* in *Oryza sativa*. *The Plant Cell* **18**, 15–28.
- Yamaguchi T, Nagasawa N, Kawasaki S, Matsuoka M, Nagato Y, Hirano HY.** 2004. The *YABBY* gene *DROOPING LEAF* regulates carpel specification and midrib development in *Oryza sativa*. *The Plant Cell* **16**, 500–509.